International Journal of Design & Nature and Ecodynamics
Vol. 20, No. 2, February, 2025, pp. 299-313
Journal homepage: http://iieta.org/journals/ijdne

Analysis of Landslide Vulnerability with Hydrothermal Alteration Using Resistivity Methods and Geological Mapping in Songgokerto Village, Batu City

Mohammad Habibiy Idmi[1], Adi Susilo[1,2*], Sukir Maryanto[1], Muwardi Sutasoma[1,2], Faridha Aprilia[1,2], Muhammad Fathur Rouf Hasan[2,3], Rony Prianto Nugraha[4]

[1] Department of Physics, Faculty of Mathematics and Natural Sciences, Brawijaya University, Malang 65145, Indonesia
[2] Center Study on Geosciences and Hazard Mitigation, Universitas Brawijaya, Malang 65145, Indonesia
[3] Department of Environmental Science, Postgraduate School, Universitas Brawijaya, Malang 65145, Indonesia
[4] Department of Engineering Science, The University of Auckland, Auckland 90210, New Zealand

Corresponding Author Email: adisusilo@ub.ac.id

https://doi.org/10.18280/ijdne.200208

Received: 6 January 2025
Revised: 11 February 2025
Accepted: 22 February 2025
Available online: 28 February 2025

Keywords:
landslide vulnerability, hydrothermal alteration, resistivity method, disaster mitigation, Batu City

ABSTRACT

Trunojoyo Street in Songgokerto Village, Batu City, is prone to frequent landslides due to its geomorphology characterized by hills and valleys, ranging from 600 to 3,337 meters above sea level. This road connects major urban and regional centers in East Java, including Batu City, Malang Regency, Kediri City, and Jombang Regency. Landslides obstruct road access, disrupting economic development and endangering road users, especially during peak tourist seasons. The dependence of Batu City's local revenue on agriculture and tourism further exacerbates the economic impact of road closures. This study employs the dipole-dipole resistivity geoelectrical method across 20 survey lines, each measuring 160 meters, with an electrode spacing of 10 meters. Moreover, the resistivity values, initially calculated in Excel, were subsequently processed using Res2Dinv with the Least Squares inversion method to produce two-dimensional pseudo cross-sections. A 2D model was used to visualize the subsurface, facilitating analysis. Results indicate low resistivity values (0–50 Ω.m), interpreted as tuff, and high resistivity values (>50 Ω.m), interpreted as volcanic breccia. Correlation of 2D models with local geological and alteration maps revealed hydrothermal alteration concentrated in zones 1 and 3 at depths of 10–35 meters. The distribution map of hydrothermal alteration is classified into two categories: Prophilitic rocks and Argillic rocks. The Prophilitic rock zone exhibits a dominant resistivity value of 1–100 Ω.m, while the Argillic rock zone has a dominant resistivity value of 100–350 Ω.m. In contrast, unaltered rocks display a dominant resistivity value exceeding 350 Ω.m. These zones correspond to areas with high landslide potential. The alteration of rocks due to continuous heat exposure reduces rock density, increasing porosity and susceptibility to landslides. Furthermore, Uniaxial Compressive Strength (UCS) and Geological Strength Index (GSI) parameter analysis indicate that continuous heat exposure has reduced rock density and increased porosity, thereby elevating the susceptibility to landslides.

1. INTRODUCTION

Indonesia has a high potential for natural disasters, ranking among the most disaster-prone countries according to the 2023 World Risk Report [1]. This vulnerability is primarily attributed to Indonesia's geographical position along the Ring of Fire [2] which exposes large areas to various natural hazards. The diversity of Indonesia's geography contributes to multiple disasters, including volcanic eruptions, earthquakes, wildfires, floods, and landslides [3].

Landslides predominantly occur in hilly and valley-dominated areas with steep slopes [4]. In addition to slope steepness, factors such as rainfall, lithology, and fault structures significantly influence landslide occurrence [5]. In hydrothermal alteration zones, landslides cause severe damage, including infrastructure destruction, ecosystem disruption, economic setbacks, and loss of life [6]. According to data from Badan Penanggulangan Bencana Daerah (BPBD) in 2016 and the Indonesian Disaster Risk Index (IDRI) in 2013, there were 357 recorded landslide events in East Java during the period of 1998–September 2016, resulting in 96 fatalities, 4 missing persons, 291 injuries, and 3,087 individuals displaced. Meanwhile, in the gateway cities of Batu and Kediri, 92 landslide occurrences were reported within a 50-day span, with a peak incidence in January through February (82.61%) [7]. Apart from causing casualties, these landslides also led to economic losses amounting to IDR 1.6 billion in 2021 [8].

The hydrothermal system in an area can lead to the formation of clay minerals in the parent rock. These minerals alter the host rock properties to exhibit low permeability, high plasticity, and reduced friction. Moreover, a hydrothermal

system weathers the rock due to the elevated temperature and pressure of hydrothermal fluids. Hydrothermal processes involving fluids with high temperatures and pressures cause deformation of the primary rock, including increased weathering, changes in density, and elevated pore pressure. The mechanism of landslides due to hydrothermal processes is usually characterized by cracks or soil deformation on the slope's surface, especially around the manifestation of hot water. Cracks or deformations occur, weakening the rock layer and accelerating ground movement due to gravity, water pressure, and additional loads [9].

The geomorphology of Batu City is dominated by hills and mountains, with elevations ranging from 600 to 3337 meters above sea level, spanning an area of 194.2 km² with a population of 213,046 [10]. These topographical features result in many areas with steep slopes. According to the Regional Disaster Management Agency (BPBD), Batu City has been identified as highly susceptible to landslides, recording 267 incidents from 2018 to 2022 [8]. One of the most vulnerable areas is the Payung region, along Trunojoyo Street in Songgokerto Village, Batu City. This road is a primary connection between Batu City and other major cities in East Java, including Malang Regency, Kediri City, and Jombang Regency.

Batu City's economy relies heavily on tourism and agriculture, both of which depend on Trunojoyo Street for accessibility [11]. Road closures caused by landslides risk human casualties and hinder economic growth in Batu City [12]. Despite mitigation efforts by the local government, including landslide-prone mapping and the installation of retaining walls, landslides continue to occur with high intensity in this area [13].

Previous studies using satellite methods to detect gravity anomalies were conducted by Hasan et al. [14] with the GGMplus gravity method and by Hasan et al. [15] who assessed and simulated potential landslides caused by rainfall intensity in Batu City during 2021. These studies indicate that Trunojoyo Street, Songgokerto Village, has a high likelihood of landslides.

The connection between high-susceptibility areas and hydrothermal alteration zones is often linked to rock alteration, which changes the mineral composition of igneous rocks. However, the detailed mechanisms and implications of hydrothermal alteration on landslide vulnerability remain underexplored, presenting a significant research gap worth investigating.

Theoretically, hydrothermal alteration causes rocks in these areas to undergo prolonged heat exposure, which affects their density [16]. Low-density rocks typically exhibit high porosity [17], allowing them to retain significant amounts of water. When the rock layers become saturated, they are prone to landslides [18]. This hypothesis underscores the need for further investigation.

The resistivity method is reliable for examining subsurface layers up to 200 meters deep [19]. It has been successfully applied in studies such as those by Susilo et al. [20] in Ponorogo to detect landslide-prone layers and Hasan et al. [21] for disaster mitigation. While effective, resistivity methods require complementary data, such as geological information, to enhance the accuracy of subsurface interpretations [22].

Geological mapping in this study aims to determine the distribution of rock units and hydrothermal alteration in the research area. Hydrothermal alteration forms deposits within hydrothermal systems. The primary components of such systems include heat sources and fluid phases, destabilizing minerals in wall rocks and forming new minerals under altered conditions [23]. This study aims to investigate the relationship between hydrothermal alteration and landslide vulnerability by combining resistivity methods and geological mapping to estimate the distribution of alteration, the distribution of resistivity values, and evaluate its role in increasing landslide susceptibility. The resistivity data obtained were correlated using the results of geological mapping and the distribution of hydrothermal alteration so that similarities and differences between the 2 methods can be found to determine the research objectives.

2. FIELD SITE STUDY

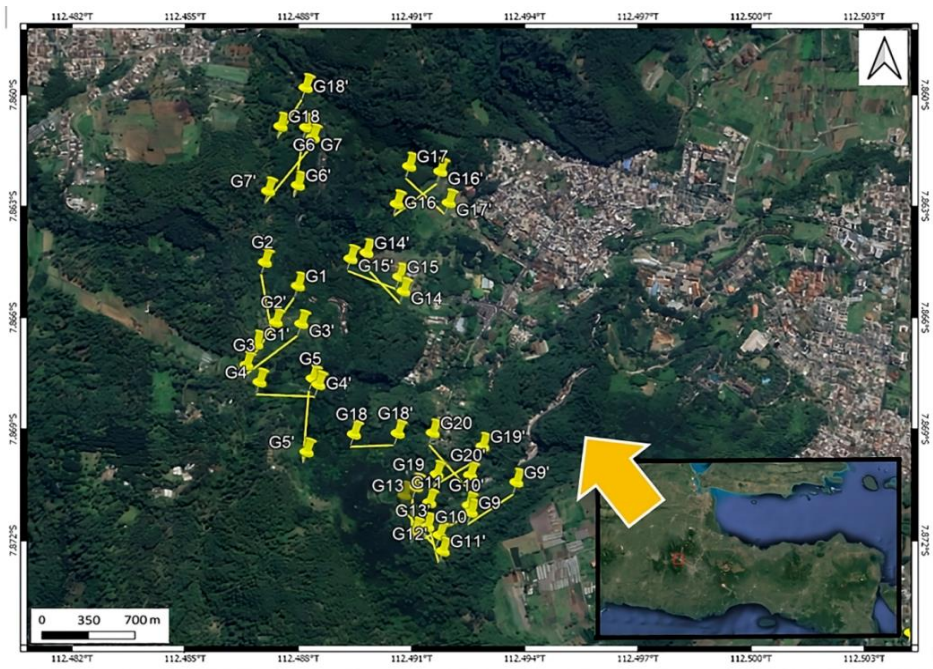

Figure 1. Survey design for the resistivity method

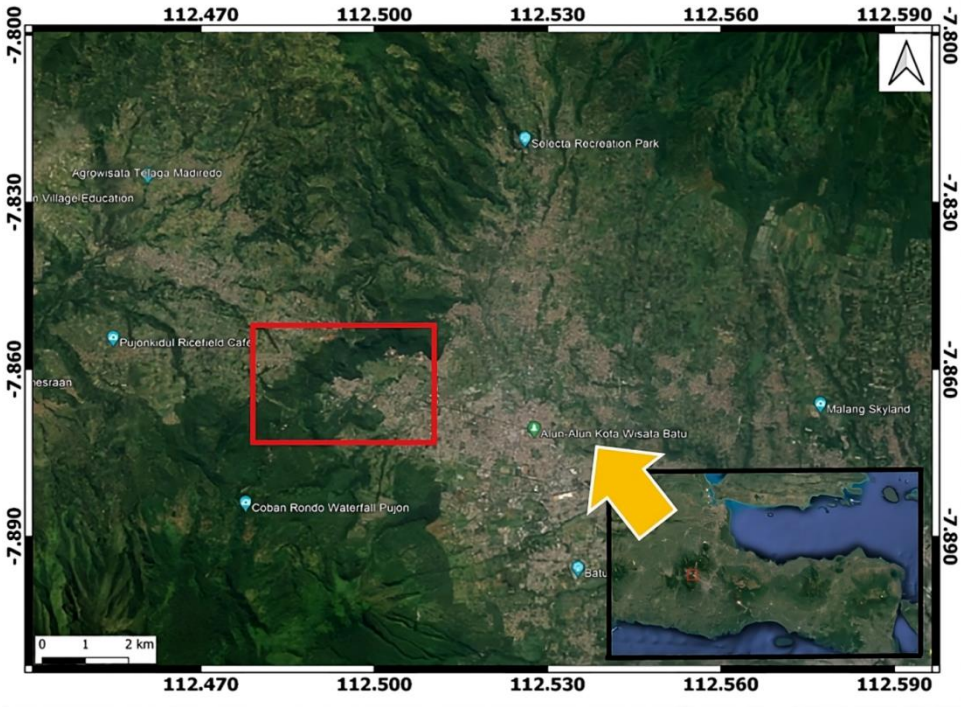

Figure 2. Geological mapping survey design

The acquisition was conducted on Trunojoyo Street, Songgokerto, Batu District, Batu City, East Java. The survey design, illustrated in Figure 1, focuses on Trunojoyo Street, which connects several regions in East Java, including Malang Regency, Kediri City, and Jombang Regency. Resistivity measurements were performed using a direct measurement method with a track length of 160 meters. The measurement method accommodated field conditions and area coverage, ensuring that each survey point was well-represented.

Geological mapping study was conducted in the same location as the resistivity method, covering an area of 1.5 × 1.5 km, as shown in Figure 2. Geological mapping was carried out to obtain a more detailed and localized distribution of rock lithology. The results serve as a reference for determining the geological framework, including geomorphology, stratigraphy, geological structures, and reconstruction of the geological history.

The primary stage of geological mapping involves direct field observation by following predetermined survey lines. This process includes observation, collection, and recording of geological data, which are then compiled and analyzed to produce a lithology distribution map [24]. Analyses include geomorphological assessments, such as quantitative evaluation of slope gradients, landform types, and formation processes. Additionally, geological structure analysis is conducted to identify the position, type, and orientation of structures encountered [25].

3. MATERIALS AND METHOD

The resistivity method is a geophysical technique that involves injecting electric current into the subsurface and measuring the resulting voltage and current, which are used to calculate resistivity values. Although this method is detailed, cost-effective, and relatively fast, it is typically suited for shallow investigations at depths of up to approximately 500 meters. Achieving penetrations beyond 500 meters requires a significantly extended survey layout, which weakens and destabilizes the current due to the larger spread length. Consequently, it is rarely employed for deep exploration. Another drawback is that it is highly susceptible to external disturbances such as the presence of water, metallic objects, cable types, electrode materials, and the accuracy of the main unit which can affect measurement results. The theoretical formulation of the geoelectrical method is based on calculating the electric potential within a given medium, induced by a current source at the Earth's surface. If a current (I) is injected into a homogeneous and isotropic subsurface layer through a single electrode, the current disperses in all directions, forming equipotential surfaces resembling hemispheres. This phenomenon is represented by Eq. (1) below [26].

$$\rho = \frac{A}{L}\frac{\Delta V}{I} \tag{1}$$

where, ρ is the resistivity (Ω.m), ΔV is the potential difference (Volt), L is Conductor Length (m), A is the Cross-sectional surface area (m^2), and I is electric current (A). The resistivity method involves several rules for electrode arrangements. These arrangements determine the geometric factor (K), which varies depending on the electrode configuration. The geometric factor (K) is a crucial parameter for estimating vertical and horizontal resistivity. In this study, the dipole-dipole configuration was selected. This configuration is effective for subsurface imaging in objects requiring relatively good vertical and horizontal penetration compared to others such as Wenner or Schlumberger. The geometric factor in the resistivity method is calculated using Eq. (2) below [27].

$$K = n(n+1)\,(n+2)\,\pi a \tag{2}$$

where, K is the geometric factor, π (pi) represents the semi-circular shape of the current distribution, a denoting the spacing between the first and second current electrodes, and n indicates the electrode spacing. Using the resistivity method,

these parameters enable the generation of a 2D pseudo resistivity distribution model. In this study, the dipole-dipole geoelectrical resistivity configuration was employed for data acquisition, with all recorded parameters subsequently processed using Microsoft Excel. Field data included the coordinates of each acquisition point, measurement elevation, the distances between current electrodes (AB) and potential electrodes (MN), the total length of the survey line, electric current (I), and the measured potential difference (ΔV). Moreover, additional contextual details such as weather conditions, measurement time, exact measurement location, and any encountered constraints were recorded to enhance the reliability of the subsequent data analysis [28].

The acquisition data are processed using Microsoft Excel to organize the dataset, calculate the geometric factor (K), and determine the apparent resistivity (ρa) [28]. The resulting apparent resistivity values can then be utilized for 2D processing in Res2Dinv, which requires input data points, electrode spacing, and resistivity values in a .dat format. The output from Res2Dinv consists of an inversion result and a 2D model. The least squares inversion method is employed, as it produces an optimal model with the smallest error. Subsequently, the 2D XYZ inversion results are processed in Google Earth to integrate topographic data, thereby yielding a 2D resistivity model that accurately represents field topography.

Geological mapping is undertaken to identify the rock units in the study area at a local scale, providing a more detailed distribution map of these units than would be available through a regional geological formation map. This process generally involves three main stages: survey design, data collection, and creating the geological map. The survey design stage is crucial, encompassing the planning of traverse routes, preparation of topographic and contour maps, and field reconnaissance to understand the terrain. Once the survey design is finalized, field data can be gathered accordingly. Key observations include slope inclination, landform, rock type, structures, hydrothermal alteration, strike, and dip. Determining each rock unit also requires sampling to evaluate characteristics such as color, structure, texture, mineral composition, grain size, packing, and rounding degree. Field measurements commonly employ instruments like a compass, GPS, and plane table, with the collected data analyzed using geological principles to produce a comprehensive map of rock unit distribution [29]. Measuring the slope using a geological compass is done by attaching the compass to the side of the plane, directing the compass needle to get the strike, and tilting the compass parallel to the plane until the dip value is obtained. Furthermore, measuring the landform or geomorphology is done using GPS to determine the height of the location, a geological compass, and a slope clinometer, making direct observation sketches such as the shape of hills, and rivers. An important process that needs to be done before determining the type of rock unit is checking the texture and mineral composition, this process consists of determining the grain size (fine, medium, coarse rocks), observing the roundness (angular, subangular, rounded), observing the packing or uniform grain size (well sorted) or not (poorly sorted). Various processes have been carried out, then a map of the distribution of rock units is made.

An integrated approach was employed to correlate resistivity results with geological mapping, aligning apparent resistivity values with geological data. This process aimed to support the identification of lithological units and alteration patterns, contributing to a more thorough interpretation of subsurface conditions. The results of apparent resistivity values that are in line with geological data are correlated with alteration distribution maps. The technique used in correlating resistivity parameters with alteration maps is to determine the dominant resistivity values that appear in different types of alteration and non-alteration areas. Then, the parameters that show results that match the resistivity, geological, and alteration parameters and the available citations can be concluded.

4. RESULT AND DISCUSSION

4.1 Literature review

The research analysis began with identifying rock formations at the study location using a geological map. The study area is included in the geological map of the Kediri sheet (Figure 3), which classifies the region into three distinct formations: the old Anjasmara volcanic rocks (Qpat), the Kawi-Butak volcanic rocks (Qpkb), and the upper quaternary volcanic rocks (Qv (Panderman)).

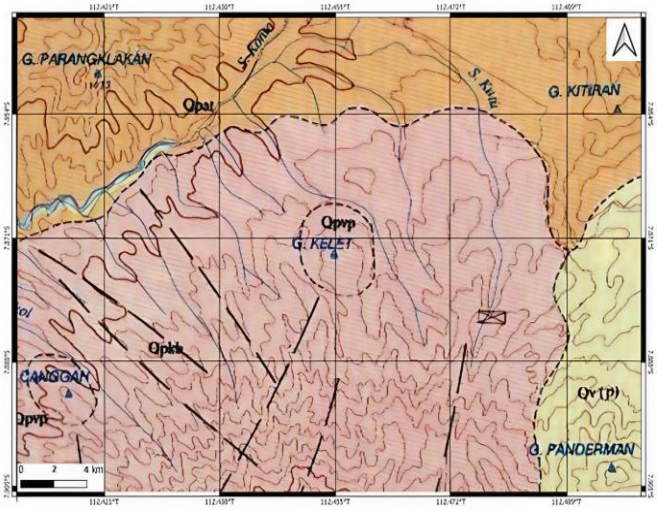

Figure 3. Regional geological map of Batu City, Kediri Quadrangle [30]

Based on the regional geological map shown in Figure 3, the Old Anjasmara Volcanic Rocks (Qpat) were formed during the Quaternary period, specifically in the Early Pleistocene. This formation comprises volcanic breccia, lava, tuff, and dikes. The Kawi-Butak Volcanic Rocks (Qpkb) were formed during the Quaternary period, specifically in the Middle to Late Pleistocene. This formation includes volcanic breccia, lava, tuff, and lahar deposits. The Upper Quaternary Volcanic Rocks (Qv (Panderman)) were formed during the Holocene. Its components consist of volcanic breccia, tuff breccia, lava, and tuff.

4.2 Geological mapping method

Geological mapping was employed to define lithological units, as regional geological maps categorize rocks based on formations, whereas local geology maps provide a more detailed classification of individual lithological units. Local geological mapping offers greater accuracy and detail,

enabling more precise interpretations alongside resistivity method analysis. The local geological mapping was conducted within the same area as the resistivity survey, and the lithological unit distribution was projected into a 2D map, as shown in Figure 4 below.

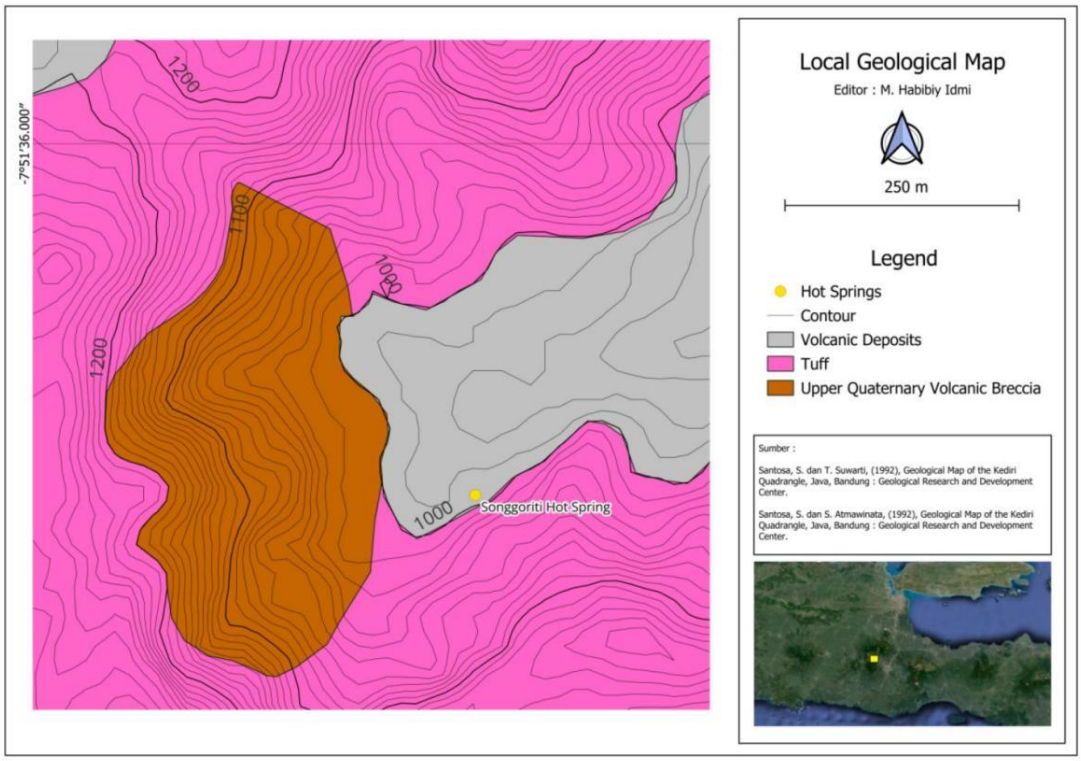

Figure 4. Local geological map

The lithological units depicted in the local geological map of Songgokerto, Batu, consist of three types: volcanic deposits, volcanic breccia, and tuff layers. These units were determined through direct field observations and classified based on the lithostratigraphic framework of the Indonesian Stratigraphy Code (1996), although the naming conventions are informal. Based on the geological mapping, the three lithological units are as follows:

1. Volcanic deposits unit

This unit is marked in gray on the map and covers a small area, primarily confined to valleys. The geomorphology of this unit is predominantly flat, featuring rice fields and small rivers. Volcanic deposits are likely from the Late Holocene period. As shown in Figure 5, these deposits consist of fine sand grains with an estimated thickness of up to 5 meters. Additionally, fragments of andesite, approximately the size of a baseball, are occasionally found.

Figure 5. Volcanic deposits unit

2. Tuff unit

This unit is predominantly found on hilltops with ridge geomorphology, dominated by pine forests. The tuff unit is marked in pink on the local geological map. It is estimated to have formed during the Pleistocene to Late Holocene period. As shown in Figure 6, the tuff is classified into two types: soft tuff and hard tuff. Additionally, several andesite rocks with diameters ranging from 2 to 3 meters are observed within this unit.

Figure 6. Tuff unit

3. Volcanic breccia unit

The last unit is volcanic breccia (Figure 7) which is found along Trunojoyo road. Volcanic breccia can be seen due to erosion of cliffs, which makes rocks in the hills or ridges visible. It is estimated to have formed during the Pleistocene to late Holocene. The form of volcanic breccia consists of various sizes of volcanic rocks such as andesite with diameters varying from 0.5 to 5 m.

Figure 7. Volcanic breccia unit

Mapping the distribution of rock alteration aims to identify areas where rocks have changed due to hydrothermal processes. Rock alteration occurs when hot fluids pass through rocks over extended periods, leading to changes in their mineral composition. The distribution of alteration is typically controlled by geological structures such as faults and fractures that are prominent in the study area.

The type of rock alteration affects the strength of the rock mass or density, this is caused by the difference in temperature of the formation of hydrothermal alteration. Based on research conducted by Wongkar and Mario in 2018 using the parameters UCS, GSI, mi H value, disturbance factor, slope height, and unit weight obtained the results of the friction angle value for each type of Argilic alteration: 44.21°, Advanced Argilic: 48.63°, and Silicic: 55.47°. The conclusion of the research that has been conducted shows that the presence of hydrothermal alteration affects the value of the friction angle in rock because it changes the minerals that make up the rock [31]. Alteration distribution map was created through direct field surveys, identifying altered rocks and their spread. In the study area, the alteration distribution is categorized into Prophilitic and Argillic, as shown in Figure 8. Meanwhile, research at the same location using UCS parameters by Hasan et al. [32] obtained the results of breccia stone 17.96 MPa, lapilli stone location 1 2.95 MPa, lapilli location 2 of 1.62 MPa, and Lapilli location 3 of 1.49 MPa. The results of the SF value test showed 1.07 <X <1.25 so that the slope condition is critical and prone to landslides.

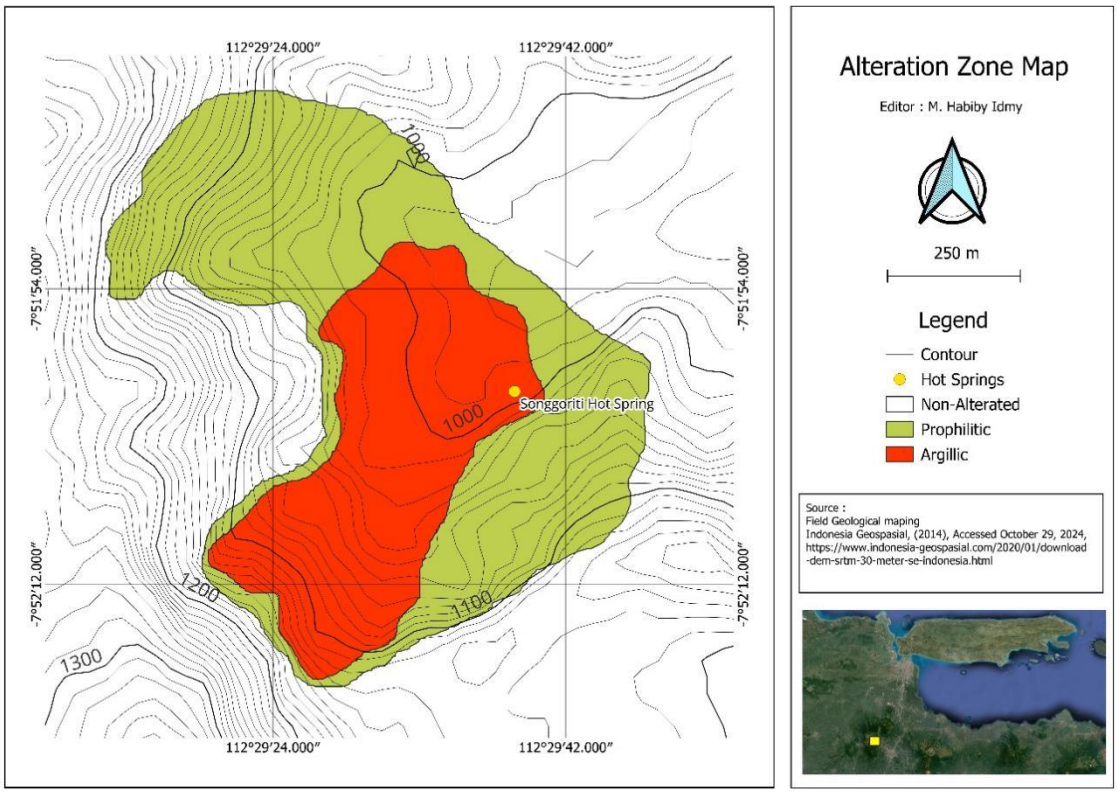

Figure 8. Alteration distribution map

The distribution of Prophilitic rock alteration is marked in green and covers a larger area than the Argillic alteration distribution. Prophilitic alteration is characterized by reddish-white rocks containing silica minerals (Figure 9(a)), with an estimated formation temperature of 120–200°C, as this alteration zone is located farther from the heat source. Meanwhile, Argillic alteration occupies 25% of the study area. The primary characteristics of this alteration include reddish-white rocks composed of silica, plagioclase, and metamorphic minerals (Figure 9(b)). This alteration typically forms in andesite rocks at temperatures of 120–220°C. The distribution of rock alteration is likely controlled by faults or fractures in the area. Further research is required to map the geological structures that influence the direction of hydrothermal activity.

4.3 Correlation between hydrothermal alteration zones and resistivity method

The resistivity method analysis is based on subsurface resistivity values projected into a 2D model. The processed results serve as a reference for determining fluid distribution. Fluid distribution is closely associated with hydrothermal alteration, where one of the main components of a hydrothermal system is the liquid phase. New mineral deposits form as thermal fluids pass through rock bodies, altering the wall rocks to align with the thermal fluid conditions. Based on

the field data processing, the 2D model interpretation is divided into four zones to simplify the analysis due to the extensive study area. The zone divisions are illustrated in Figure 10 below.

Figure 9. (a) Prophilitic altered rock, (b) Argillic altered rock

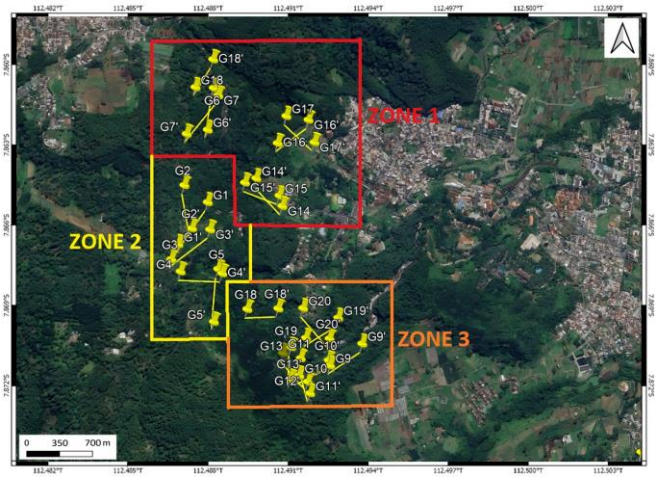

Figure 10. (a) Zone 1, (b) Zone 2, (c) Zone 3

The determination of zoning is based on the distribution of rock alteration types, where the resistivity path is spread across 3 different zones: the Prophylitic, Argillic, and non-altered alteration zones illustrated in Figure 11. To enhance the scientific rigor, geological justification for the zoning could include factors such as variations in lithology, structural controls like faults and fractures, and the distribution of hydrothermal alteration. These geological characteristics can provide a more robust explanation for the observed resistivity patterns and ensure that the zoning reflects meaningful subsurface features rather than mere spatial proximity.

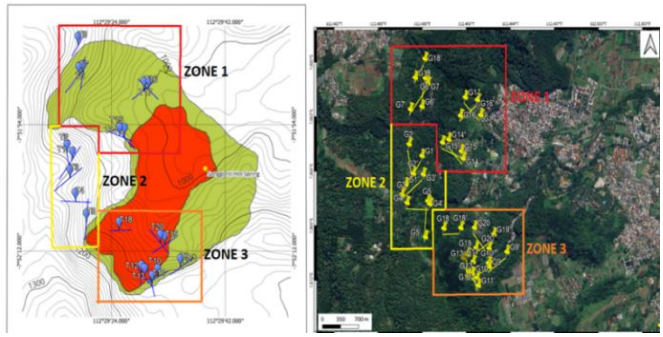

Figure 11. Correlation of zones on the (a) Alteration map and (b) Survey design

1. Zone 1: Located in the northernmost part of the study area, comprising tracks L6, L7, L8, L14, L15, L16, and L17
2. Zone 2: Located in the central region, including tracks L1, L2, L3, L4, and L5.
3. Zone 3: Found in the southernmost area, containing the largest number of tracks totaling seven: L9, L10, L11, L12, L13, L18, and L19.

This zoning approach reduces the area size for analysis and simplifies the interpretation of 2D models while facilitating correlation with rock alteration distribution. The study of hydrothermal alteration distribution is based on resistivity values ranging from 0 to 50 Ω.m, which are interpreted as tuff layers with high porosity. Rocks with high porosity can retain larger amounts of fluid, making fluid presence a primary indicator of hydrothermal alteration.

1. **Low Resistivity:** Ranging from 0 to 50 Ω.m, represented by dark blue to green, interpreted as tuff layers.
2. **High Resistivity:** Greater than 50 Ω.m, represented by yellow to purple, interpreted as volcanic breccia layers.

The obtained resistivity values have different dominant resistivity value patterns, this is in line with the resistivity value zone or rock alteration distribution. Zone 1 consists of 7 tracks in the Prophylitic alteration zone with dominant resistivity values ranging from 1 - 100 Ω.m which can be seen in Figure 12 with dark blue to light green colors. Zone 2 is in a non-altered area with a very high dominant resistance of >350 Ω.m marked in dark red in Figure 13, this is most likely due to the absence of altered rocks in this zone. Zone 2 is in a non-altered area. Then zone 3 is in argillic alteration with a dominant resistance value of 100-350 Ω.m marked in yellow to orange in Figure 14.

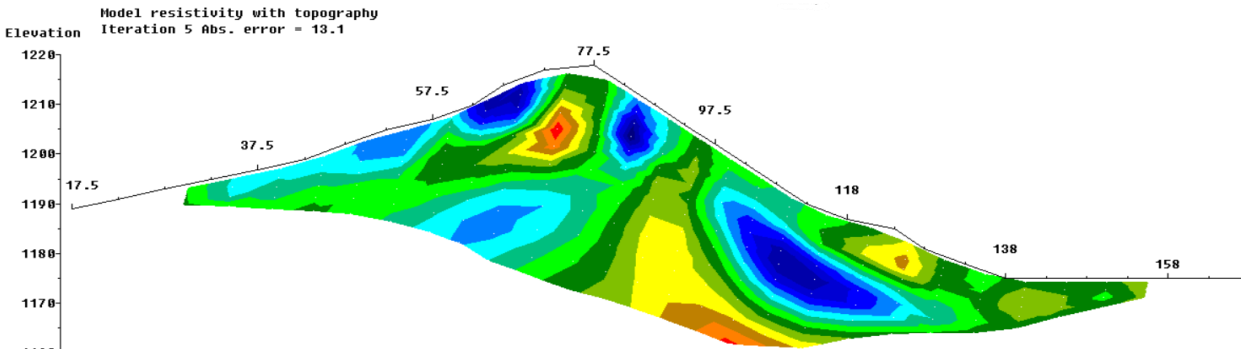

(a)

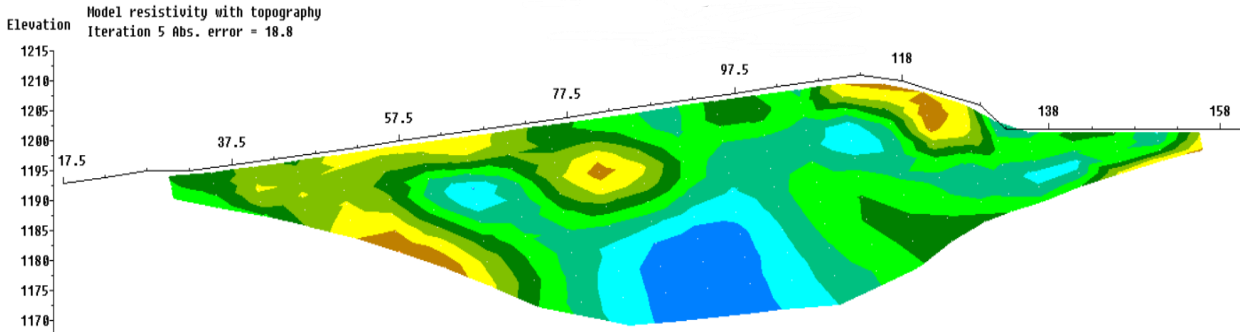
Model resistivity with topography
Iteration 5 Abs. error = 18.8
Elevation
1215
1210
1205
1200
1195
1190
1185
1180
1175
1170
17.5
37.5
57.5
77.5
97.5
118
138
158

(b)

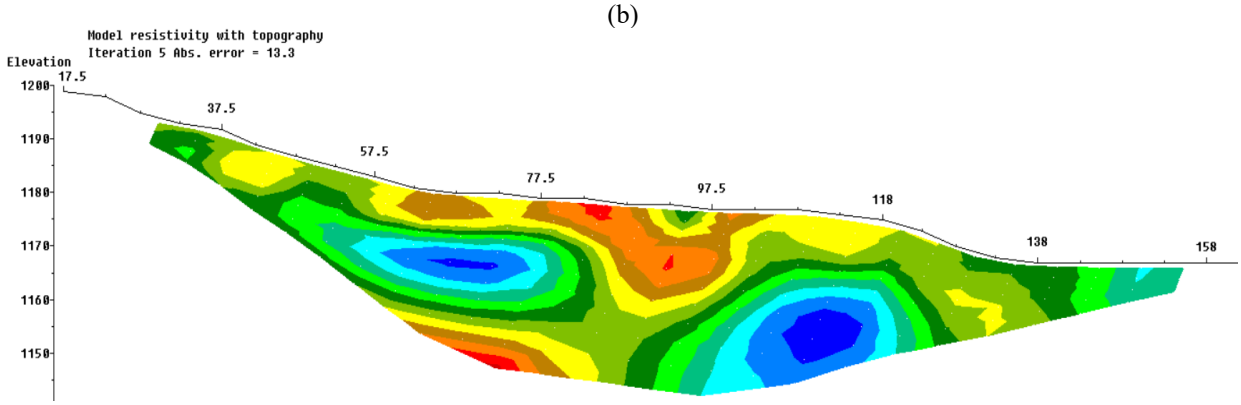
Model resistivity with topography
Iteration 5 Abs. error = 13.3
Elevation
1200
1190
1180
1170
1160
1150
17.5
37.5
57.5
77.5
97.5
118
138
158

(c)

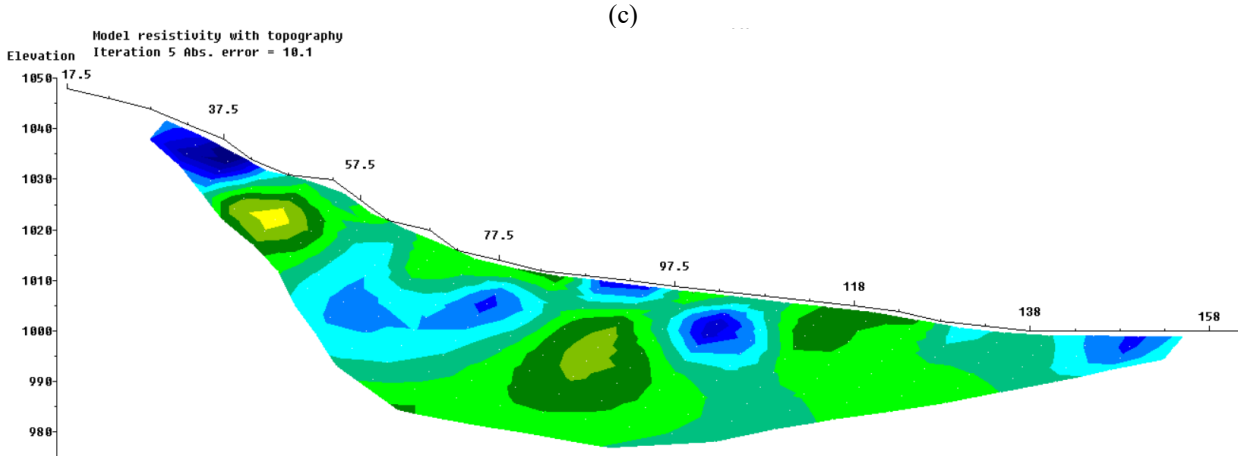
Model resistivity with topography
Iteration 5 Abs. error = 10.1
Elevation
1050
1040
1030
1020
1010
1000
990
980
17.5
37.5
57.5
77.5
97.5
118
138
158

(d)

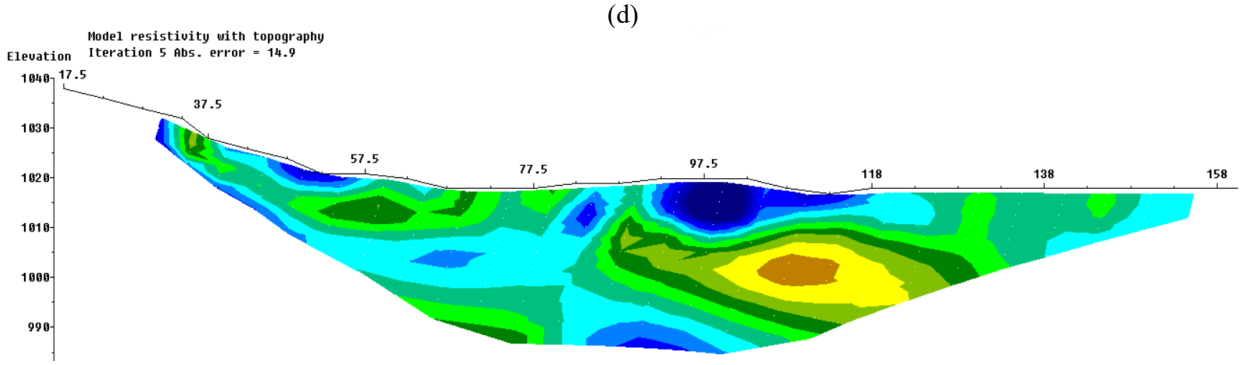
Model resistivity with topography
Iteration 5 Abs. error = 14.9
Elevation
1040
1030
1020
1010
1000
990
17.5
37.5
57.5
77.5
97.5
118
138
158

(e)

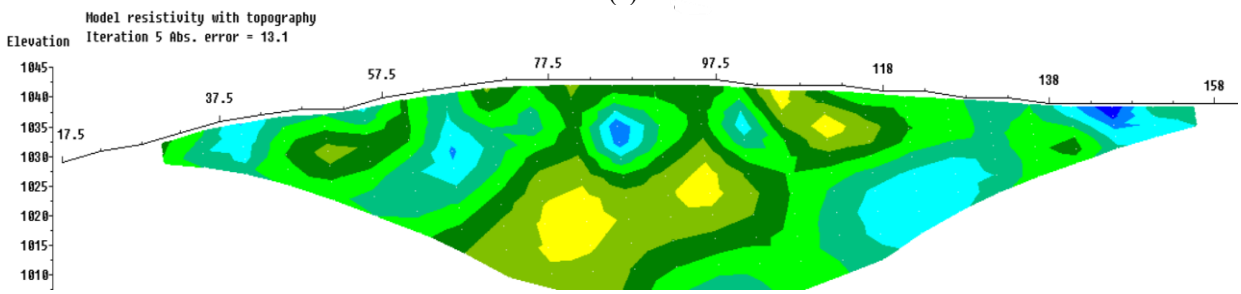
Model resistivity with topography
Iteration 5 Abs. error = 13.1
Elevation
1045
1040
1035
1030
1025
1020
1015
1010
17.5
37.5
57.5
77.5
97.5
118
138
158

(f)

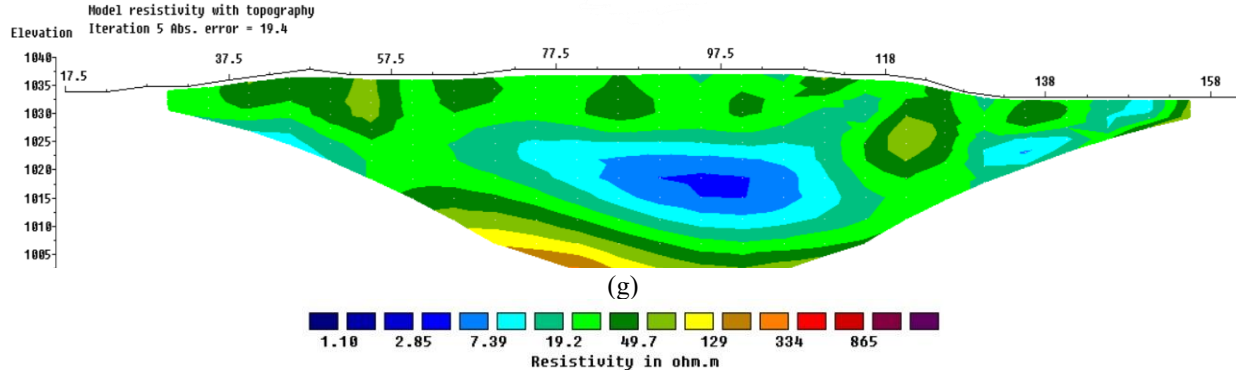

(g)

Figure 12. Zone 1 of (a) Track 6, (b) Track 7, (c) Track 8, (d) Track 14, (e) Track 15, (f) Track 16, dan (g) Track 17

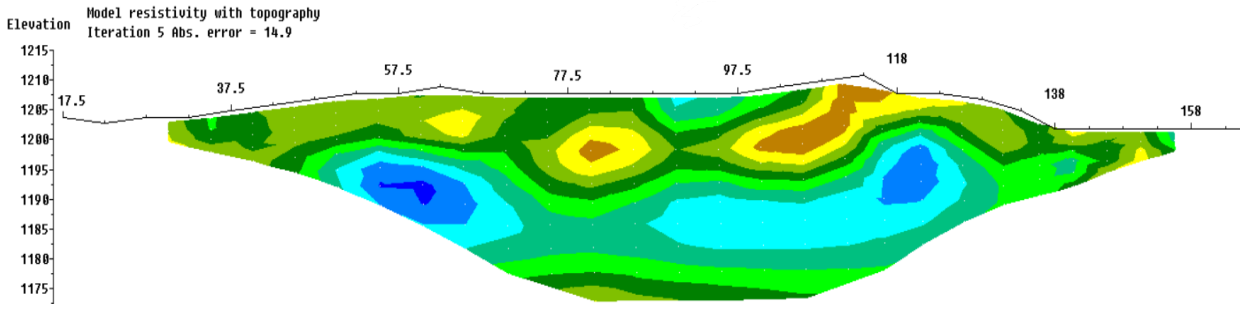

(a)

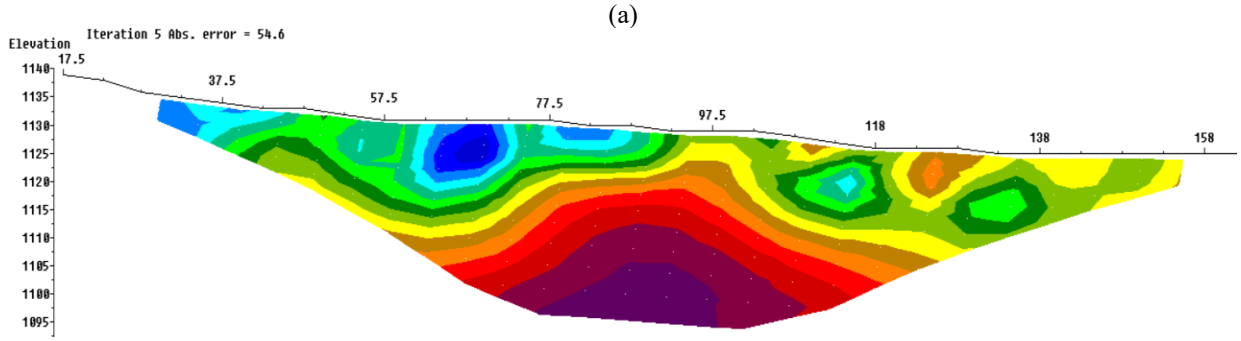

(b)

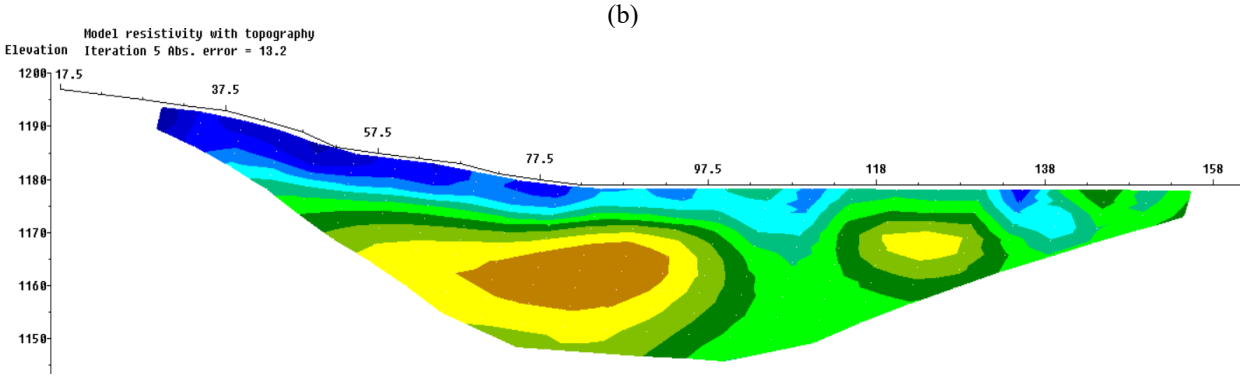

(c)

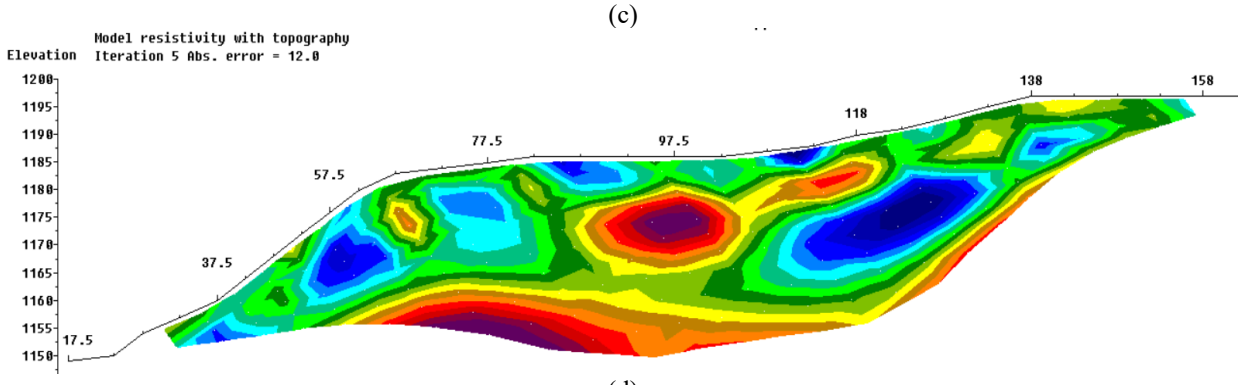

(d)

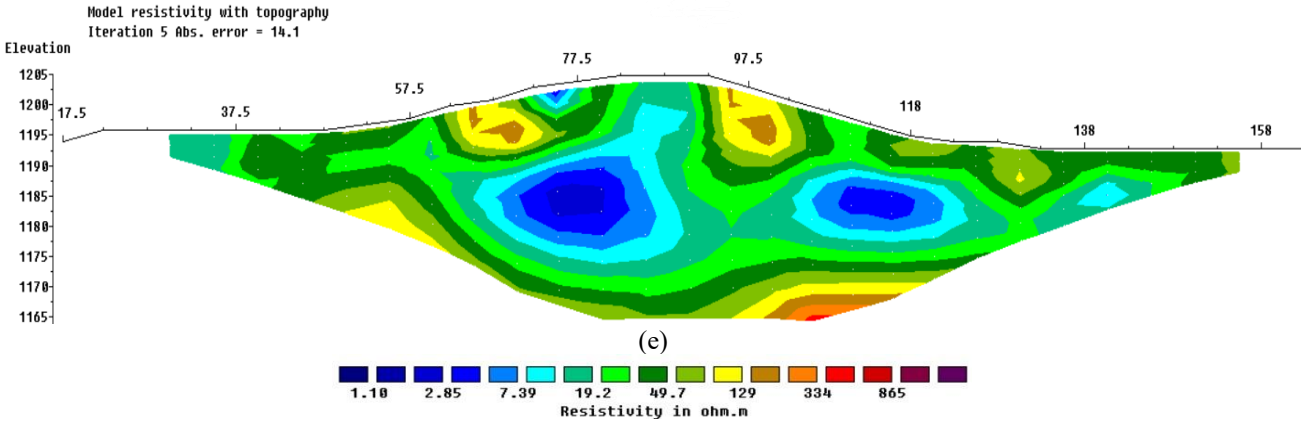

(e)

Figure 13. Zone 2 of (a) Track 1, (b) Track 2, (c) Track 3, (d) Track 4, dan (e) Track 5

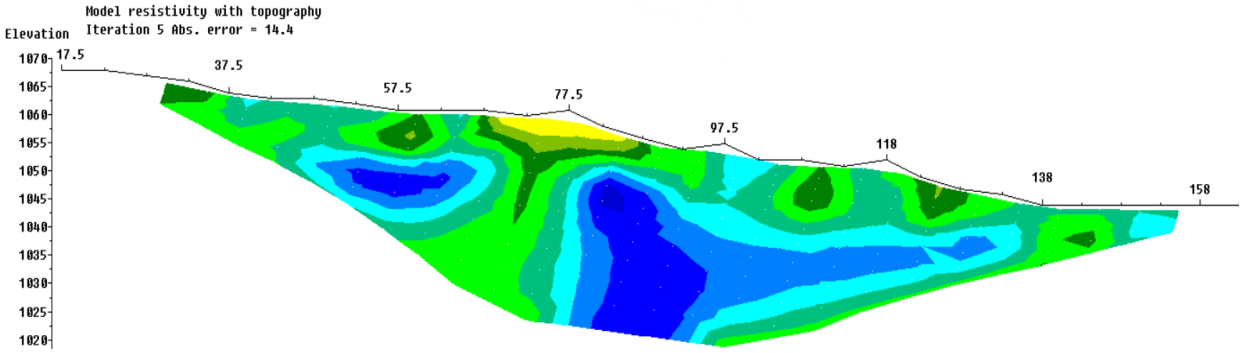

(a)

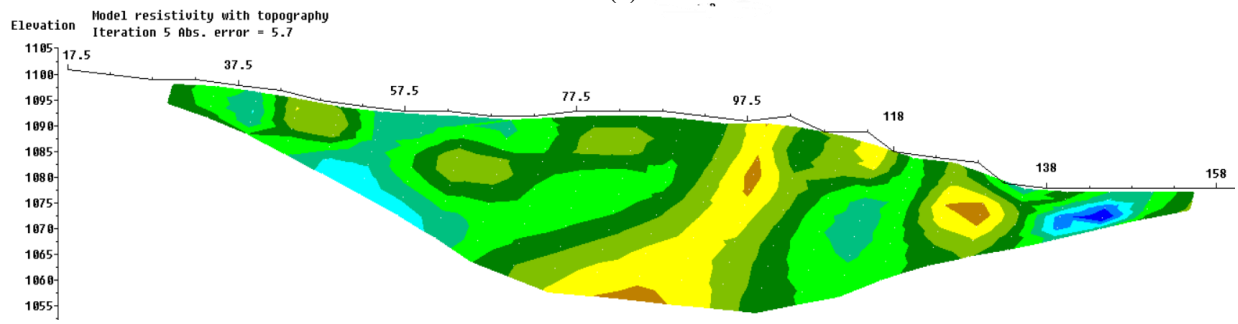

(b)

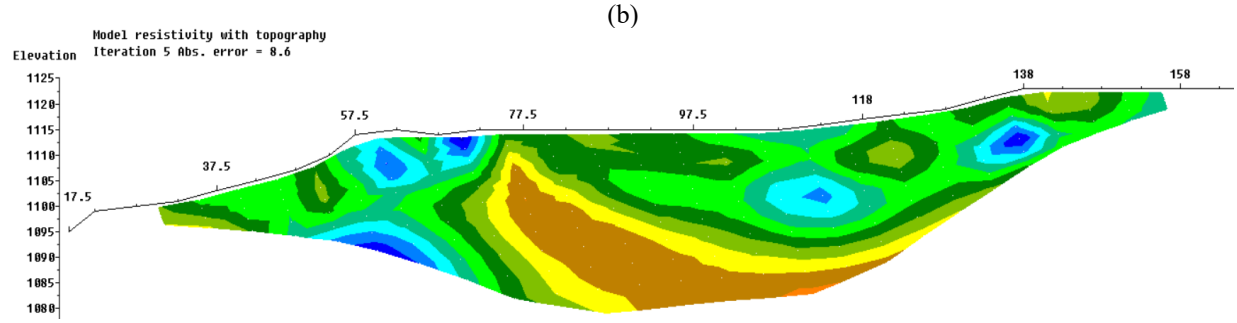

(c)

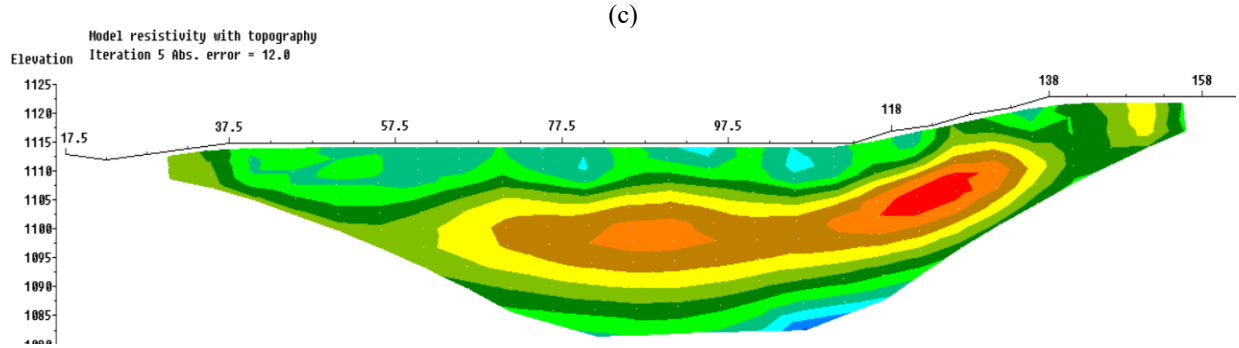

(d)

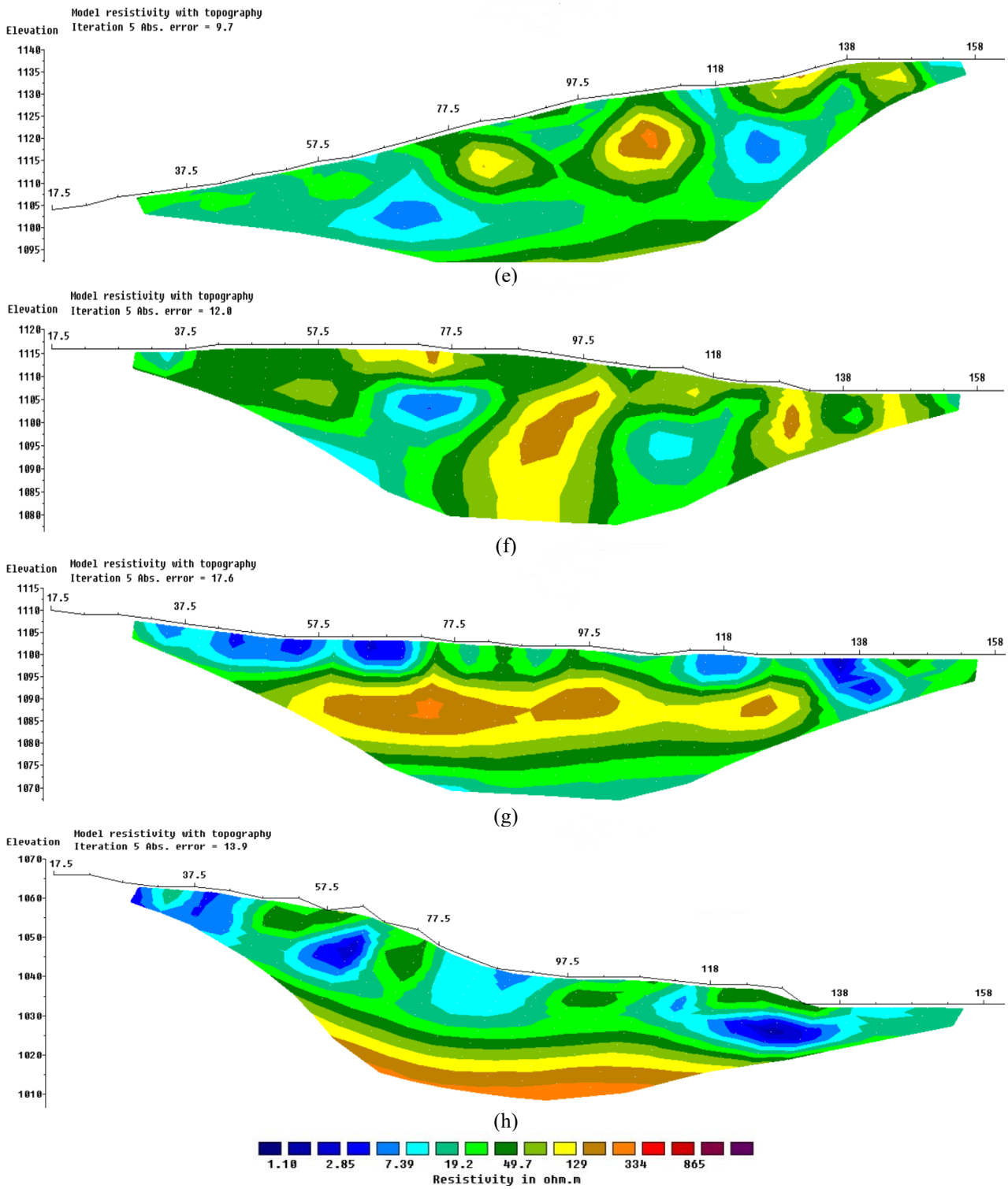

Figure 14. Zone 3 of (a) Track 9, (b) Track 10, (c) Track 11, (d) Track 12, (e) Track 13, (f) Track 18, (g) Track 19, and (h) Track 20

The interpretation of resistivity values indicates the potential for hydrothermal alteration in tracks with resistivity values ranging from 0 to 50 Ω.m. Hydrothermal alteration is represented by dark blue to green colors at depths of approximately 10 to 35 meters. The 2D resistivity modeling effectively illustrates subsurface resistivity distribution in the study area. The correlation between the distribution of altered rocks and resistivity values demonstrates consistent results. The analysis of the 2D model reveals that hydrothermal alteration is concentrated in Zone 1, and Zone 3. This finding is further validated by the hydrothermal distribution map, which identifies Prophilitic and Argillic rock alterations in these zones.

Zone 2, represented by tracks L1, L2, L3, L4, and L5, has indications of hydrothermal alteration distribution. However, field observations did not find rocks altered by hydrothermal processes, suggesting that this area is characterized by groundwater sources instead. The rock alteration and geological mapping results support the conclusion that Zone 2 is influenced by groundwater rather than hydrothermal alteration. This area predominantly comprises volcanic tuff and volcanic breccia with high porosity, and numerous water

springs were observed in the region (Figure 15).

Figure 15. Cold water springs in Zone 2

Resistivity strongly correlates with landslide activity, as it reflects a rock's capacity to conduct electrical current. Low resistivity indicates that the rock more readily conducts electrical current, a property influenced by its composition, water content, and density. Consequently, rocks with lower resistivity are likely to contain more water than those exhibiting higher resistivity. Landslides typically occur in rocks with high water saturation, since water filling the pore spaces reduces the cohesive force between particles. Once the gravitational driving force surpasses the resisting force, slope failure becomes inevitable. According to the study, low resistivity values ranging from 0 to 50 Ω.m are interpreted as tuff. Tuff layers possess high porosity, allowing water to infiltrate the rock matrix and destabilize it, thereby increasing the likelihood of landslides.

The relation between soil parameters and resistivity was conducted empirically with regression between soil resistivity and the number of landslide activities. The purpose of the regression analysis was to see the pattern of the relationship between landslide activity and resistivity values. The total number of landslide activity events that passed through the resistivity path was 22, with 15 occurring in the alteration zone and 7 occurring outside the alteration zone. Then the average resistivity value in the alteration zone ranges from 100 Ω.m while outside the alteration zone ranges from 100 to 350 Ω.m. Regression was carried out between the number of landslide events with small resistivity values at the landslide location, the Multiple R results in the alteration zone were very strong ($R^2 = 0.89$), then the non-alteration zone was strong ($R^2 = 76$). The graph of landslide activity with resistivity values shows that landslides often occur at low resistance values (Figure 16).

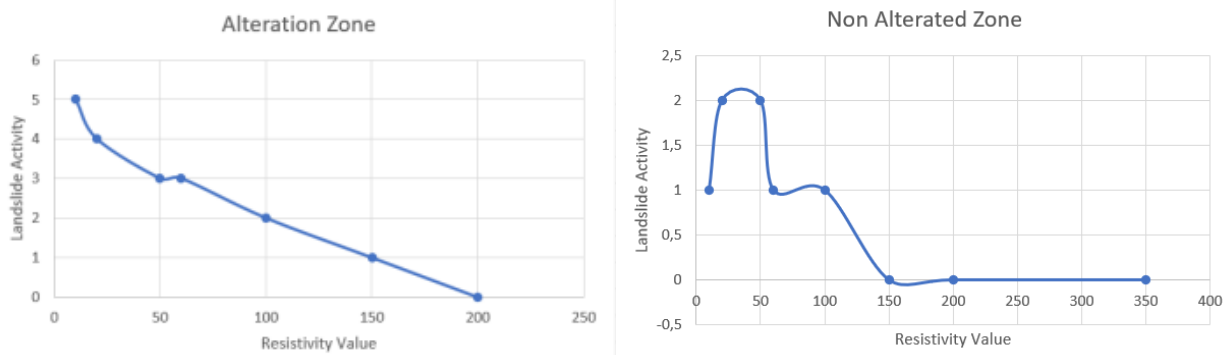

(a) (b)

Figure 16. Landslide activity graph with resistivity values of (a) Alteration zone and (b) Non alteration zone

4.4 Correlation between hydrothermal alteration zones and resistivity method

The correlation between the dominant resistivity value of each zone with the distribution of hydrothermal alteration that has been discussed shows that the zone containing hydrothermal alteration has a small dominant resistivity value compared to the non-altered zone. Zones 1 and 2 have a significantly different dominant resistivity value, while based on the geological mapping that has been carried out, shows that Zones 1 and 2 have similar rock units, namely volcanic breccia. Then Zone 3 tuff rock units so it is natural that zones 1 and 2 have dominant resistivity values that are different from Zone 3. The difference in dominant resistivity values in the alteration zone is an indication that alteration can change rock density. Changes in rock density can be an early indication of the cause of landslides in this area.

Previous studies by Hasan et al. [14] using the magnetic method identified areas along Trunojoyo Street with high landslide susceptibility, attributed to low-density rocks at various landslide points. Additionally, BPBD data highlights landslide occurrences concentrated in areas marked in red in Figure 17. When correlated with the rock alteration distribution map, landslide-prone zones align with areas of hydrothermal alteration. This suggests that hydrothermal alteration in rocks can contribute to landslide susceptibility. Hydrothermal alteration alters the composition of minerals within rocks, reducing their density. Lower-density rocks are more prone to landslides because their resisting forces diminish compared to driving forces.

Based on the analysis, while rainfall is generally considered a major factor in increasing landslide risk, prior research by Hasan et al. [15] showed that the Songgokerto area in Batu City, despite having lower rainfall than other regions, exhibits the highest landslide rate. This discrepancy suggests that landslides in the area are not primarily driven by rainfall. Further studies on seismic activity indicate that Songgokerto is surrounded by several volcanoes, with the Arjuna-Welirang volcanic system recording five "emission earthquakes," each having amplitudes of 1–2 mm and durations of 71.2 seconds. Meanwhile, Mount Kawi and Mount Anjasmoro are seismically inactive. Since the research site is approximately 17.6 km from Arjuna-Welirang mountain range, volcanic seismicity is presumed to have only a minor effect on

landslides. According to the regional geological map, there are no active faults in this locale, with the nearest active fault situated roughly 10 km from Songgokerto, Batu City. These findings collectively imply that external factors such as volcanic seismicity, fault movement, and rainfall exert only a limited influence on the occurrence of landslides in this region.

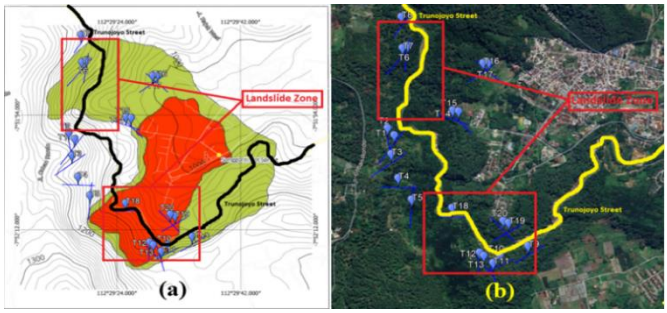

Figure 17. Correlation between (a) Rock alteration distribution and (b) Landslide-prone zones

In 2024, from the survey conducted, a total of 59 landslide incidents occurred (Figure 18). Although Zone 1 has undergone alteration, its landslide vulnerability remains low, with only 18 incidents. This outcome is likely attributed to its gentle slope inclination, which is not steep enough to produce a significant driving force. Conversely, Zone 3 shows a higher landslide frequency, reaching 28 incidents, possibly due to its steep slope of 70–80 degrees and the presence of low-density rock caused by alteration. Zone 2, which recorded fewer landslides (13 incidents), has slopes of 80–90 degrees but is dominated by high-density volcanic breccia and shows no evidence of alteration. In addition to steep slopes and rock alteration, geological structures such as faults also contribute to landslides. Consequently, further investigation using magnetic and gravity methods is needed to comprehensively map the geological structures in the study area.

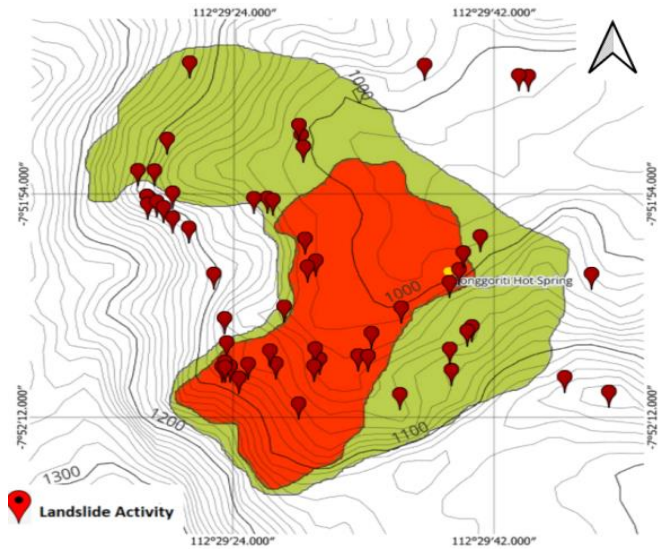

Figure 18. Landslide activity

The study conducted provides a clear overview of the relationship between hydrothermal alteration and landslide activity. Given that frequent landslides pose a serious threat to public safety, the Batu City government must adopt effective mitigation measures. Although retaining walls and cliff reinforcements have already been constructed, landslides have continued to occur within a few months, suggesting that the primary causes remain unresolved. One recommended solution is to establish a well-designed drainage system, particularly for hot water runoff. Additionally, installing support columns at depths exceeding 25 meters that penetrating hard bedrock could help stabilize soil displacement caused by ground movement. Finally, implementing robust land-use policies is crucial, as the conversion of forested areas into agricultural fields significantly raises the risk of soil erosion during rainfall.

5. CONCLUSIONS

The 2D resistivity distribution model provides information on the subsurface resistivity anomalies up to 35 meters. Resistivity values are categorized into two groups: low resistivity (0–50 Ω.m), interpreted as tuff, and high resistivity (>50 Ω.m), interpreted as volcanic breccia. The correlation of the hydrothermal alteration map with the resistivity method shows that Zone 1 is in the Prophylitic alteration zone with a dominant resistance value ranging from 1 - 100 Ω.m. Zone 2 is in a non-altered area with very high dominant resistance which is >350 Ω.m. Then Zone 3 is in argillic alteration with a dominant resistance value of 100-350 Ω.m. Zones 1 and 2 have a dominant resistivity value difference that is much different from similar rock units, namely volcanic breccia and zone 3 tuff rock units. The difference in dominant resistivity values in the alteration zone is an indication that alteration can change rock density. Changes in rock density can be an early indication of the cause of landslides in this area. The correlation between landslide activity and hydrothermal alteration shows that many landslides occur in altered zones, particularly Zone 1 and Zone 3. Of the total 55 recorded landslide events, Zone 1 experienced 11, while Zone 3 accounted for 20 events. These landslides result in substantial harm, both in terms of loss of life and economic impact, thereby necessitating government-led mitigation measures. Such measures include constructing water drainage systems, installing concrete retaining piles at depths exceeding 25 meters, and developing land management regulations. Ensuring the effectiveness of these mitigation efforts requires transparent collaboration among local communities, government authorities, and disaster management agencies.

ACKNOWLEDGMENT

The author would like to thank the Ministry of Education, Culture, Research and Technology of the Republic of Indonesia for financial support through the BIMA Master's Thesis Grant program with contract No.: 045/E5/PG.02.00.PL/2024.

REFERENCES

[1] Frege, I.A., Bradshaw, S., Funk, C., Kienzl, P., Küsters, K., Masuch, L., Nasreen, M., Radtke, K., Schneider, S., Thielbörger, P., Weller, D., Wiegers, O., Yaman, D.K., Zennig, K. (2023). WorldRiskReport 2023 Focus: Diversity. Berlin: Bündnis Entwicklung Hilft.

[2] Hamilton, W.B. (1979). Tectonics of the Indonesian

region. US Government Printing Office. https://doi.org/10.3133/pp1078
[3] Masum, M., Akbar, M.A. (2019). The pacific ring of fire is working as a home country of geothermal resources in the world. IOP Conference Series: Earth and Environmental Science, 249(1): 012020. https://doi.org/10.1088/1755-1315/249/1/012020
[4] Riestu, I.M., Hidayat, H. (2023). Landslide susceptibility mapping using random forest algorithm and its correlation with land use in Batu City, Jawa Timur. IOP Conference Series: Earth and Environmental Science, 1127(1): 012017. https://doi.org/10.1088/1755-1315/1127/1/012017
[5] Sulaiman, M.S., Nazaruddin, A., Salleh, N.M., Abidin, R.Z., Miniandi, N.D., Yusoff, A.H. (2019). Landslide occurrences in Malaysia based on soil series and lithology factors. International Journal of Advanced Science and Technology, 28(18): 1-26.
[6] Hadmoko, D.S., Lavigne, F., Samodra, G. (2017). Application of a semiquantitative and GIS-based statistical model to landslide susceptibility zonation in Kayangan Catchment, Java, Indonesia. Natural Hazards, 87: 437-468. https://doi.org/10.1007/s11069-017-2772-z
[7] Wahyudianto, E. (2018). Analysis and risk study on landslide hazard frequency at road corridor of Batu City–Kediri Regency border. Journal of the Civil Engineering Forum, 4(3): 265-275.
[8] Central Statistics Agency of Batu City. (2022). Batu City Disaster Event Data (Data Kejadian Bencana Kota Batu). Batu City Government.
[9] Silwal, B.R., Ota, K., Yoshida, K. (2024). Effects of hydrothermal activity and weathering in the active fault area: Formation of large landslide and landslide dam lake, Lake Nakatsuna, Nagano, Japan. Natural Hazards, 120: 9057-9091. https://doi.org/10.1007/s11069-024-06567-4
[10] Central Statistics Agency of Batu City. (2021). Official Statistics News of the 2020 Population Census Results of Batu City (Berita Statistik Resmi Hasil Sensus Penduduk 2020 Kota Batu). Batu City Government.
[11] Kodir, A. (2018). Tourism and development: Land acquisition, achievement of investment and cultural change (Case study tourism industry development in Batu City, Indonesia). GeoJournal of Tourism and Geosites, 21(1): 253-265.
[12] Meijer, J.R., Huijbregts, M.A.J., Schotten, K.C.G.J., Schipper, A.M. (2018). Global patterns of current and future road infrastructure. Environmental Research Letters, 13(6): 064006. https://doi.org/10.1088/1748-9326/aabd42
[13] Oleinik, P., Kuzmina, T., Kuzmin, K. (2018). Effective technology for strengthening natural slopes and artificial structures. MATEC Web of Conferences, 193: 02040. https://doi.org/10.1051/matecconf/201819302040
[14] Hasan, M.F.R., Susilo, A., Suryo, E.A., Agung, P.A. M., Idmi, M.H., Suaidi, D.A., Aprilia. F,. (2024). Mapping of landslide potential in Payung, Batu City, Indonesia, using Global Gravity Model Plus (GGMplus) data as landslide mitigation. Iraqi Geological Journal, 57(1A): 159-168. https://doi.org/10.46717/igj.57.1A.13ms-2024-1-24
[15] Hasan, M.F.R., Susilo, A., Suryo, E.A., Agung, P.A. M., Pratiwie, D.L., Dewi, N.M. (2024). Assessment and simulation of potential landslide caused by the rainfall intensity in Batu City during 2021. IOP Conference Series: Earth and Environmental Science, 1314(1): 012017. https://doi.org/10.1088/1755-1315/1314/1/012017
[16] Mathieu, L. (2018). Quantifying hydrothermal alteration: A review of methods. Geosciences, 8(7): 245. https://doi.org/10.3390/geosciences8070245
[17] Bohnsack, D., Potten, M., Pfrang, D., Wolpert, P., Zosseder, K. (2020). Porosity–permeability relationship derived from Upper Jurassic carbonate rock cores to assess the regional hydraulic matrix properties of the Malm reservoir in the South German Molasse Basin. Geothermal Energy, 8: 12. https://doi.org/10.1186/s40517-020-00166-9
[18] Okamoto, T., Matsuura, S., Larsen, J.O., Asano, S., Abe, K. (2018). The response of pore water pressure to snow accumulation on a low-permeability clay landslide. Engineering Geology, 242: 130-141. https://doi.org/10.1016/j.enggeo.2018.06.002
[19] Fajana, A.O. (2020). Groundwater aquifer potential using electrical resistivity method and porosity calculation: A case study. NRIAG Journal of Astronomy and Geophysics, 9(1): 168-175. https://doi.org/10.1080/20909977.2020.1728955
[20] Susilo, A., Fitriah, F., Sunaryo, Rachmawati, T.A., Suryo, E.A. (2020). Analysis of landslide area of Tulung subdistrict, Ponorogo, Indonesia in 2017 using resistivity method. Smart and Sustainable Built Environment, 9(4): 341-360. https://doi.org/10.1108/SASBE-06-2019-0082
[21] Hasan, M.F.R., Salimah, A., Susilo, A., Rahmat, A., Nurtanto, M., Martina, N. (2022). Identification of landslide area using geoelectrical resistivity method as disaster mitigation strategy. International Journal on Advanced Science, Engineering and Information Technology, 12(4): 1484-1490.
[22] Loke, M.H., Rucker, D.F., Chambers, J.E., Wilkinson, P.B., Kuras, O. (2021). Electrical resistivity surveys and data interpretation. In: Encyclopedia of Solid Earth Geophysics, pp. 344-350. https://doi.org/10.1007/978-3-030-58631-7_46
[23] Eichelberger, J. (2020). Distribution and transport of thermal energy within magma–hydrothermal systems. Geosciences, 10(6): 212. https://doi.org/10.3390/geosciences10060212
[24] Lisle, R.J. (2020). Geological Structures and Maps: A Practical Guide. United Kingdom: Butterworth-Heinemann.
[25] Taija, T., Lucy, W. (2024). An introduction to geological mapping of our world and others. Geological Society, 541: 1-17. https://doi.org/10.1144/SP541-2023-201?ref=pdf&rel=cite-as&jav=VoR
[26] Telford, W.M., Telford, W.M., Geldart, L.P., Sheriff, R.E. (1990). Applied Geophysics. Cambridge: Cambridge University Press.
[27] Singh, U., Sharma, P.K. (2022). Study on geometric factor and sensitivity of subsurface for different electrical resistivity Tomography Arrays. Arabian Journal of Geosciences, 15(7): 560. https://doi.org/10.1007/s12517-022-09844-3
[28] Sunaryo, Susilo, A. (2017). Seepage zone identification at Sutami Dam by means of geoelectrical resistivity data. IOP Conference Series: Earth and Environmental Science, 75(1): 012011. https://doi.org/10.1088/1755-1315/75/1/012011

[29] Siler, D.L., Faulds, J.E., Hinz, N.H., Dering, G.M., Edwards, J.H., Mayhew, B. (2019). Three-dimensional geologic mapping to assess geothermal potential: examples from Nevada and Oregon. Geothermal Energy, 7: 1-32. https://doi.org/10.1186/s40517-018-0117-0

[30] Atmawinata S., Santoso S. (1992). Geological Map of the Kediri Quadrangle, Java. Geological Research and Development Centre, Bandung, Indonesia. https://onesearch.id/Record/IOS1.INLIS000000000141917.

[31] Wongkar, W., Mario, F. (2018). Effect of hydrothermal alteration type on rock mass strength (Pengaruh jenis alterasi hidrotermal terhadap kekuatan massa batuan). Prosiding Temu Profesi Tahunan PERHAPI, 1(1): 307-312. https://www.prosiding.perhapi.or.id/index.php/prosiding/article/view/31/32.

[32] Hasan, M.F.R., Frastika, M.Y., Agung, P.A.M., Susilo, A., Suryo, E.A., Zaika, Y., Juwono, A.M., Zulaikah, S. (2024). Influence of rock weathering and saturation on compressive strength and slope stability: A Uniaxial test analysis. International Journal of Safety & Security Engineering, 14(1): 145-153. https://doi.org/10.18280/ijsse.140114

NOMENCLATURE

n	Number of Layers
I	Current (Ohm)
V	Voltage (Volt)
K	Geometric Factor
P1	Symbol of Potential Electrode (meter)
P2	Symbol of Potential Electrode (meter)
C1	Symbol of Current Electrode (meter)

Greek symbols

π	Phi
α	Distance Between Electrodes (meters)
ρa	Apparent Resistivity Value (Ohm)
Ω	Measured Resistivity Value (Ohm)
μ	dynamic viscosity, kg. $m^{-1}.s^{-1}$